



Topographic Effects on the Seismic Coefficient and Earthquake-Induced Permanent Displacement of Earth Slopes

Jian Song^(✉) and Yufeng Gao

Key Laboratory of Ministry of Education for Geomechanics and Embankment Engineering, Hohai University, Nanjing 210098, China
jiansonghh@163.com

Abstract. Topographic irregularities have found to considerably affect the amplitude and frequency content of ground motions, but this effect is not included in current pseudo-static and displacement-based methods of seismic slope stability analysis. In this study, two-dimensional (2D) seismic response of step-like slopes under vertically propagating in-plane shear waves (SV waves) is assessed to investigate the topographic effects on seismic coefficient and permanent displacement of earth slopes. The analyses are performed for slopes with different heights, inclinations, soil types subject to artificial input motions with various frequencies. The decoupled method is adopted to separately calculate the seismic response of slopes and the permanent displacements. The slip surface of slopes and the characteristics of sliding mass are firstly derived through static stability analysis, and the seismic coefficient of sliding mass is then evaluated by assuming no sliding scenario occurs. The permanent seismic displacements are finally computed by the Newmark method. The one-dimensional (1D) seismic analysis is also performed for the sliding mass, and the results are compared with those from the 2D analysis to provide some insights into the topographic effects on the assessment of the seismic stability of earth slopes. It is found that the conventionally used ratio of slope height to the wavelength may not consistently perform well to describe the topographic effects for slopes over a rigid bedrock, where the soil layer amplification is dominant. The ratio of the fundamental site period to the predominant frequency of the input motion can be used to characterize the topographic effects on the seismic coefficient and earthquake-induced permanent displacement of earth slopes. In addition, the 1D analysis does not consistently provide conservative results compared with 2D analysis for the full cover sliding cases.

Keywords: Earth slopes · Earthquake-Induced landslides · Topographic effects
Seismic coefficient · Newmark displacement

1 Introduction

Newmark's [1] original methodology is generally referred to as rigid-block analysis. For deformable sliding mass, the dynamic response of the sliding mass should be taken into account. To this end, the decoupled method is widely used in which the dynamic

response analysis is firstly performed to compute the horizontal seismic coefficient time history by assuming no failure surface [2], and then the sliding displacement is computed by the rigid-block analysis with the horizontal seismic coefficient time history (multiplies g) as the input motion. Both two-dimensional (2D) finite element analysis [3] and one-dimensional (1D) soil column [4] can be used to model this dynamic response, while the 1D analysis is more commonly used in previous studies. Topographic effects on the amplitude and frequency content of earthquake ground motions have been well observed in various studies and destructive earthquakes [5, 6]. However, most previous studies on the topographic effects mainly focused on estimating the modification in ground motions along the slope surface and few attempts to the slope stability. It is therefore important to understand the topographic effects on the seismic slope stability and to investigate the adequacy of 1D analysis to accurately predict the horizontal seismic coefficient of a 2D slope.

In this study, we investigate the topographic effects on the seismic coefficient and permanent displacement of earth slopes by comparing both 1D and 2D results. Several slope models with various characteristics are analyzed to examine the interaction between topographic amplification and soil layer amplification and its influence on the evaluation of seismic slope stability.

2 Analysis Methodology

2.1 Critical Slip Surface and Horizontal Yield Coefficient

As an initial step, the critical slip surface and the horizontal yield coefficient (k_y) of slopes were determined through pseudo-static analyses using FLAC [7]. The k_y was obtained to result in a factor of safety equal to 1.0 by incrementally increasing the horizontal component of gravitational acceleration of the numerical model. The sliding surface can be characterized by searching the positions where have a large shear strain increment. The Mohr–Coulomb model was used in the pseudo-static analysis. The physical and mechanical properties used for the soil materials are presented in Table 1, and the slope models analyzed in this study are listed in Table 2. Figure 1 shows an example of the determined critical slip surface for different types of soil. The sandy slope (cohesionless soil) are generally associated with a shallower slip surface while a deeper sliding surface occurs for the clayey slope (cohesive soil). The influence of the difference in sliding mass geometry on the seismic coefficient and earthquake-induced permanent displacement need to be clarified.

2.2 Dynamic Response and Horizontal Seismic Coefficient of Sliding Mass

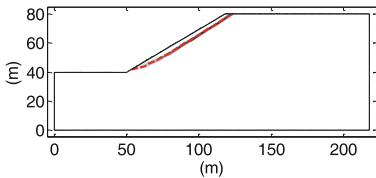
The dynamic response of the sliding mass is represented by the average horizontal acceleration within the sliding mass, i.e., the seismic coefficient time history (k). This is illustrated in Fig. 2(a), and can be given by:

Table 1. Physical and mechanical parameters of soil.

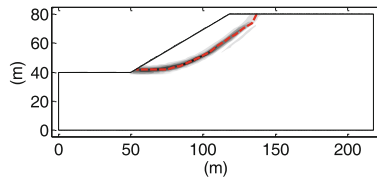
Parameters	Stiff clay	Dense sand	Relative stiff clay	Relative dense sand
Dry density (kg/m^3)	2000	2000	1800	1800
Poisson's ratio	1/3	1/3	1/3	1/3
Shear wave velocity V_s (m/s)	400	400	200	200
Cohesion (kPa)	50	2	26	0.5
Friction angle ($^\circ$)	25	42	18	37
Dilation angle ($^\circ$)	0	0	0	0

Table 2. Slope model parameters.

Soil type	Slope height, H (m)	Slope inclination, i ($^\circ$)	Soil layer thickness, Z (m)	Factor of safety	Yield coefficient (k_y)	Sliding mass depth (m)	Soil column depth (m)
Stiff clay	40	15	100	2.677	0.37	16.5	84.4
Stiff clay	40	30	100	1.549	0.22	11.7	85.1
Stiff clay	40	45	100, 150, 200, 250	1.119	0.07	10.7	86.3, 134.3, 186.3, 234.3
Stiff clay	40	45	Half-space	1.119	0.07	10.7	Half-space
Stiff clay	20	30	80	2.141	0.41	7.5	73.6
Relative stiff clay	20	30	80	1.369	0.16	7.1	72.5
Dense sand	40	30	100	1.549	0.15	3.0	82.2
Dense sand	20	30	80	1.701	0.20	1.7	71.2
Relative dense sand	20	30	80	1.365	0.11	0.8	71.3



(a) Slope with dense sand



(b) Slope with stiff clay

Fig. 1. Critical slip surface of sandy and clayey slopes ($H = 40$ m, $i = 30^\circ$, $V_s = 400$ m/s).

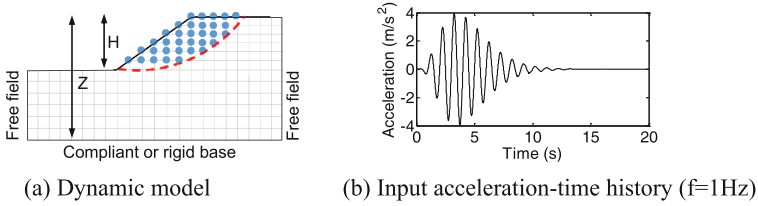


Fig. 2. Dynamic analysis model of slopes and the input ground motions used in this study.

$$k(t) = a_{avg}(t) = \frac{\sum_{\text{slidingmass}} m_i a_i(t)}{\sum_{\text{slidingmass}} m_i g} \quad (1)$$

where m_i and a_i are the mass and acceleration of nodal points within the sliding mass. The length of the dynamic model is 1000 m for $H = 40$ m, and is 500 m for $H = 20$ m. The base of the mesh is assumed to be a rigid boundary to consider the interaction between the soil layer and topographic effects. A compliant base where a quiet absorbing boundary is used at the base of model for one case of the homogeneous half-space. The free-field boundaries are applied to both the lateral boundaries to minimize reflections from the lateral boundaries (Fig. 2a). We use Chang's time histories with an amplitude of 0.4 g and dominant frequencies range from 0.2 to 10 Hz as inputs (Fig. 2b). The soil is modelled as a linear viscoelastic material with a target damping ratio of 5% using Rayleigh damping. The element size is taken as 4 m for $V_s = 400$ m/s and 2 m for $V_s = 200$ m/s (a tenth of the minimum wavelength of input motion) to assure the accurate representation of wave transmission through the model.

3 Topographic Effects on the Seismic Coefficient

3.1 Verification of Numerical Accuracy

The numerical accuracy of the model is verified with that from [5]. The slope model studied in [5] is in a homogenous half-space. The comparison result is shown in Fig. 3, where the ratio of acceleration amplitude in the slope crest from 2D analysis and 1D analysis versus various normalized frequencies (i.e., ratio of slope height to the wavelength, H/λ) is shown. The results agree well with each other at all H/λ values.

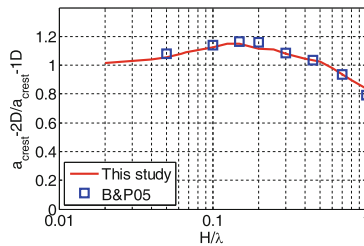


Fig. 3. A comparison of the result from this study with [5] ($i = 45^\circ$, homogeneous half-space).

3.2 Parametric Analysis of Slope Geometry

Slope Inclination. The amplitude ratio of acceleration in slope crest (a_{crest}) and seismic coefficient (multiplies g) from 2D analysis to the peak acceleration of the input motion versus normalized frequencies H/λ for various slope inclinations is shown in Fig. 4. Also shown is the amplitude ratio of seismic coefficient from fully 2D analysis (k_{max-2D}) and 1D analysis (k_{max-1D}) using the averaged depth of the sliding mass and the soil column of the sliding mass to the bottom boundary. We can see the amplification is larger for crest acceleration than k . This is expected and consistent with [8] because the amplification is reduced from the crest to bottom of slope surface, and k is the averaging result of the acceleration of sliding mass. Note that the difference between the crest acceleration and k is dependent on the normalized frequencies H/λ . The maximum amplification occurs at H/λ equal to 0.1. This corresponds to the first natural period of the 1D soil column behind the crest (equal to $4Z/V_s = 1.0$ s), which means that soil layer amplification is dominant. In addition, the maximum amplification in 2D k_{max} increases slightly as increasing the slope inclination, with a maximum amplification near 500%. Also can be seen from the figure is that the 1D result is not consistently conservative. There are some cases (H/λ between about 0.15 and 0.25) that the 2D k_{max} is larger than 1D k_{max} , and the maximum ratio also increases slightly with increasing the slope inclination (with a maximum ratio of 1.4 for $i = 45^\circ$).

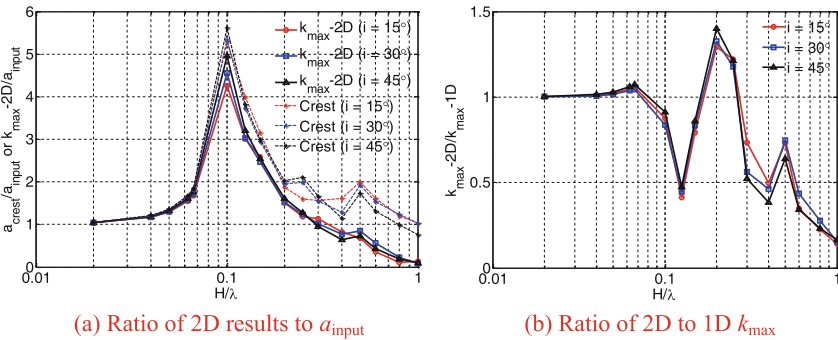


Fig. 4. Amplification of a_{crest} and k_{max} of the sliding mass from 1D and 2D analysis for various slope inclinations (stiff clay, $H = 40$ m, $V_s = 400$ m/s and $Z = 100$ m).

Slope Height. Figure 5 shows amplification of the acceleration amplitude in slope crest and the 2D and 1D k_{max} for different slope heights. We can see the normalized frequency at the maximum amplification is different for the two slope heights. The amplification ratios shift to larger H/λ values for $H = 40$ compared to $H = 20$ m. Therefore, for slopes in a rigid bedrock, the normalized frequency H/λ may not be consistently good for describing the topographic effects. In this case, the soil layer and topographic effects are coupled together. The maximum ratio of 2D to 1D k_{max} is similar for different slope heights.

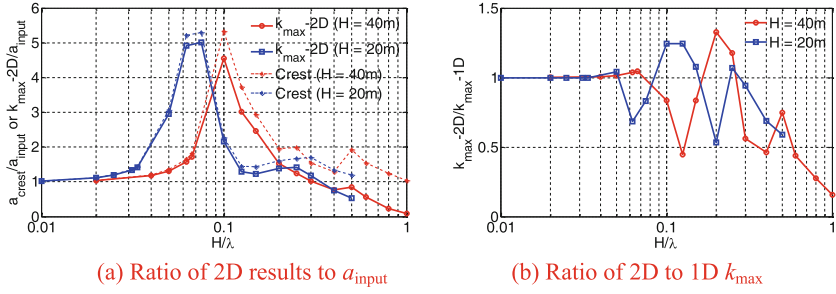


Fig. 5. Amplitude amplification of a_{crest} and k_{max} of the sliding mass from 1D and 2D analysis for various slope heights (stiff clay, $i = 30^\circ$, $V_s = 400$ m/s, $Z = 100$ and 80 m).

3.3 Parametric Analysis of Soil Layer

Soil Type. As an example shown in Fig. 1, the sandy slopes are generally associated with a shallower slip surface while a deeper sliding surface occurs for the clayey slope. Therefore, the influence of this difference in the sliding mass geometry on the seismic coefficient is investigated, as shown in Fig. 6. Observe that the amplification in crest acceleration and 2D k_{max} is consistent for two soil types. This is related to the distribution of the coupled amplification (topographic and soil layer) within slope. The amplification reduces significantly from the crest to the bottom of the slope surface, but it is similar from the slope surface to some deeper bodies along the horizontal direction. The slight difference observed in the ratio of 2D to 1D k_{max} is likely the result of the different sliding mass depth in the 1D analysis (Table 2).

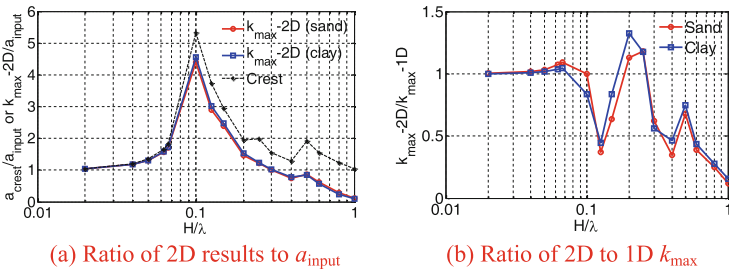


Fig. 6. Amplification of a_{crest} and k_{max} of the sliding mass from 1D and 2D analysis for different soil types ($H = 40$ m, $i = 30^\circ$, $V_s = 400$ m/s, $Z = 100$ m).

Shear Wave Velocity of Soil. Figure 7 shows the amplification of the acceleration amplitude in slope crest and k_{max} of the sliding mass from 1D and 2D analysis for different clay soils (different shear strengths and shear wave velocities). The amplification in crest acceleration and k_{max} is similar for the two clay soils, although there is a slight difference observed in the ratio of 2D to 1D k_{max} . Therefore, when there is a rigid bedrock beneath the earth slope, the stiffness and strength of the soil have little

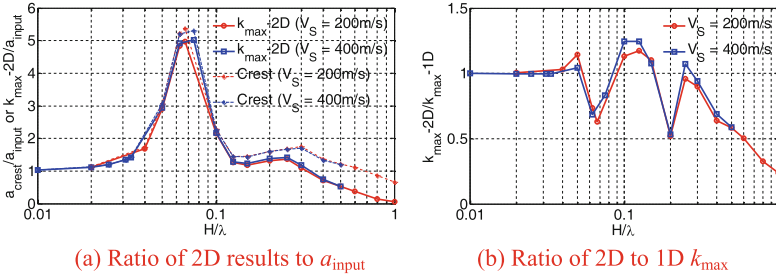


Fig. 7. Amplification of a_{crest} and k_{max} of the sliding mass from 1D and 2D analysis for soils with various shear wave velocities (clay, $H = 20$ m, $i = 30^\circ$, $Z = 80$ m).

influence on the k estimation. Note that this may be different for an elastic bedrock, in which the shear wave velocity ratio between soil and bedrock is important.

Thickness of Soil Layer. Figure 8 shows the amplification of the acceleration amplitude in slope crest and k_{max} of the sliding mass from 1D and 2D analysis for different soil layer thicknesses, along with the result of the homogenous half-space. Similar to the observation in different slope heights, the maximum amplification ratio is not at a constant H/λ value, and there is a shift to larger H/λ values for a thinner soil layer. In addition, the topographic effects is more prominent for a thinner soil layer from the ratio of 2D to 1D k_{max} . The amplification in a homogenous half-space is much lower than the case of a rigid bedrock. Although the assumption of a rigid bedrock could have aggravated the interaction between topographic and soil layer effects, it is recommended that a more realistic elastic bedrock base is used to examine these coupled effects on the assessment of seismic landslide hazard.

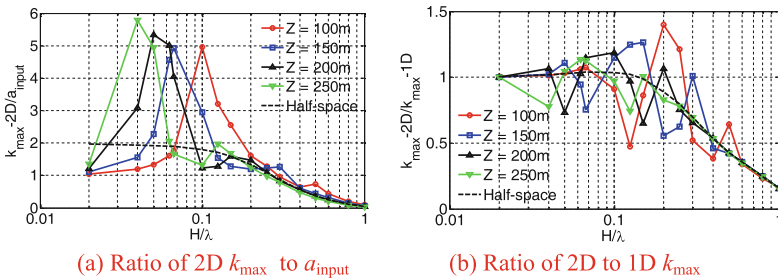


Fig. 8. Amplification of k_{max} of the sliding mass from 1D and 2D analysis for various soil layer thicknesses (stiff clay, $H = 40$ m, $i = 45^\circ$, $V_s = 400$ m/s).

4 Topographic Effects on the Permanent Displacement

One important observation above is that H/λ may not be consistently good to describe the topographic effects for slope in a rigid bedrock. Therefore, we use the period ratio, defined as the ratio of the natural period of the soil column in 1D analysis to the

predominant frequency of input motion to characterize the topographic effects, as shown in Fig. 9. We can see that the topographic effects can be well determined by the period ratio. A slight amplification is observed at a period ratio range of approximate 0.4–0.7, and another significant amplification occurs at a period ratio range of 1.2–2.2. The maximum mean ratio is 1.2 for k_{\max} and 1.6 for permanent displacement. At other period ratios, topographic de-amplification relative to 1D analysis occurs. Also interesting to note that there are two de-amplification valleys at the first natural period and 1/3 of first natural period (i.e., the second natural period) of the soil layer and one de-amplification peak at 1/4 of first natural period. It is noted that all the identified critical slip surfaces for the homogeneous earth slopes in this study are full cover sliding through the slope surface, where the 1D analysis was considered to provide a significant conservative estimate of seismic coefficient and permanent displacement [8].

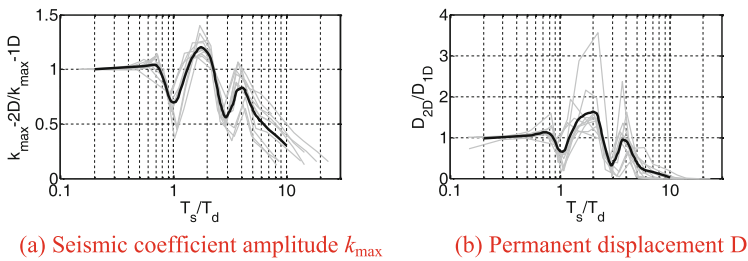


Fig. 9. k_{\max} and D from 1D and 2D analysis versus period ratio (gray thin lines are the results for different slope models and the black thick line represents the mean value of the ratio).

5 Conclusions

This paper presents some decoupled analysis results to investigate the topographic effects on the estimation of seismic coefficient and earthquake-induced permanent displacement of earth slopes. A rigid bedrock base is used to consider the interaction between the soil layer and topographic effects. We found that the conventionally used normalized frequency H/λ may not consistently perform well to describe the topographic effects for slope in a rigid bedrock, where the soil layer amplification is dominant. The period ratio of the natural period of the soil column with an averaged thickness from the sliding mass to the bottom boundary to the predominant frequency of the input motion can be used to characterize the topographic effects on the seismic coefficient and earthquake-induced permanent displacement of earth slopes. In addition, the 1D analysis does not consistently provide conservative results compared with 2D analysis for the full cover sliding cases.

Acknowledgements. This research has been supported by the National Natural Science Foundation of China (Grant No. 41602280 and 41630638), National Key Basic Research Program of China (Grant No. 2015CB057901), National Key Research and Development Program of China (Grant No. 2016YFC0800205), China Postdoctoral Science Foundation (Grant No. 2016M601708), the Fundamental Research Funds for the Central Universities in China

(Grant No. 2016B01114), a Project Funded by the Priority Academic Program Development of Jiangsu Higher Education Institutions (PAPD).

References

1. Newmark, N.M.: Effects of earthquakes on dams and embankments. *Geotechnique* **15**, 139–159 (1965)
2. Chopra, A.K.: Earthquake response of earth dams. *J. Soil Mech. Found. Div. ASCE* **93**(2), 65–81 (1967)
3. Makdisi, F.I., Seed, H.B. Simplified procedure for estimating dam and embankment earthquake induced deformations. *J. Geotech. Eng. Div. ASCE*, 849–867 (1978)
4. Rathje, E.M., Antonakos, G.: A unified model for predicting earthquake-induced sliding displacements of rigid and flexible slopes. *Eng. Geol.* **122**(1), 51–60 (2011)
5. Bouckovalas, G.D., Papadimitriou, A.G.: Numerical evaluation of slope topography effects on seismic ground motion. *Soil Dyn. Earthq. Eng.* **25**(7), 547–558 (2005)
6. Tripe, R., Kontoe, S., Wong, T.K.C.: Slope topography effects on ground motion in the presence of deep soil layers. *Soil Dyn. Earthq. Eng.* **50**(7), 72–84 (2013)
7. Itasca Consulting Group. *FLAC: fast Lagrangian analysis of continua* (2005)
8. Rathje, E.M., Bray, J.D.: One- and two-dimensional seismic analysis of solid-waste landfills. *Can. Geotech. J.* **38**(4), 850–862 (2001)